Journal of Industrial and Engineering Chemistry 73 (2019) 142–151

Contents lists available at ScienceDirect

Journal of Industrial and Engineering Chemistry

journal homepage: www.elsevier.com/locate/jiec

Human hair keratin-based hydrogels as dynamic matrices for facilitating wound healing

So Yeon Kim[a,b,1], Bong Joo Park[c,1], Yunki Lee[d], Na Jeong Park[d], Kyung Min Park[e], Yu-Shik Hwang[a,**], Ki Dong Park[d,*]

[a] Department of Maxillofacial Biomedical Engineering and Institute of Oral Biology, School of Dentistry, Kyung Hee University, Seoul 02447, Republic of Korea
[b] Department of Dental Hygiene, College of Health Science, Cheongju University, Cheongju 360-764, Republic of Korea
[c] Department of Electrical and Biological Physics and Institute of Biomaterials, Kwangwoon University, Seoul 01897, Republic of Korea
[d] Department of Molecular Science and Technology, Ajou University, Suwon 16499, Republic of Korea
[e] Divivion of Bioengineering, College of Life Sciences and Bioengineering, Incheon National University, Incheon 22012, Republic of Korea

ARTICLE INFO

Article history:
Received 3 December 2018
Received in revised form 16 January 2019
Accepted 17 January 2019
Available online 4 February 2019

Keywords:
Polymeric hydrogels
Hair keratin
Wound healing
Keratinocyte
Migration
Epithelial-Mesenchyme Transition

ABSTRACT

Recently, human hair-derived keratin protein has been recognized as biomaterial with high potential due to its excellent bioactivity and biocompatibility. Here, we designed human hair-derived keratin-based *in situ* cross-linkable hydrogels that can serve as a dynamic matrix for the enhanced wound healing. We demonstrated that our developed the keratin-based hydrogels accelerated re-epithelization and wound healing process in a full-thickness animal. Also, we investigated the molecular mechanism underlying the enhanced wound healing. In conclusion, our study proposes that human hair-derived keratin-based hydrogels with excellent bioactivity have great potential for use as a wound healing material, along with its other biomedical applications.

Introduction

Polymeric hydrogels, which is hydrophilic three-dimensional (3D) network, have attracted substantial attention for wound management because the hydrophilic matrices provide a moist environments, absorb wound exudates, and protect the wound sites against external infection [1,2]. In particular, *in situ* cross-linkable hydrogels are widely utilized as dynamic matrices for facilitating wound healing because of good tissue integration with irregular defect sites and patient compliance [3–9]. While various kinds of synthetic and natural polymers have been used to create the hydrogel materials, there is a growing interest in the development of advanced hydrogel materials for enhanced wound healing processes *in vivo*.

A wound is caused by the disruption of the integrity of skin tissues, resulting in damage or loss in some or all of the skin layers. Wound healing is a complex biological process mediated by various cellular and matrix components to reestablish the integrity of the damaged tissue or to replace lost tissue [10,11]. Over the past several decades, various biological and synthetic biomaterials have been developed to accelerate the wound healing process. Of the various biological and synthetic biomaterials, collagen, a major protein in the matrix component of dermis, has been widely used for wound care in multiple physical formats, such as membrane, scaffold and hydrogel [12,13]. In the wound healing process, it was reported that collagen showed hemostatic function and chemotactic function for fibroblast and macrophages and provided matrix for the ingrowth of tissue [14]. Although collagen in biomaterials used for wound healing is derived from various animals such as cow, pig and rat, the exogenous collagen is thought to have a similar biological function in wound healing to endogenous collagen with regard to the evolutionarily conserved peptide sequence between animal-derived collagen and human collagen. However, exogenous xenogenic collagen has been known to trigger local immune response including allergic reaction via the reactivity of circulating antibodies against alpha 1 and alpha 2 polypeptides of collagen, which may cause improper or impaired wound healing [15,16]. Such an immune reaction is known to also

* Corresponding author at: Department of Molecular Science and Technology, Ajou University, 5 Woncheon-dong, Yeongtong-gu, Suwon 443-749, Republic of Korea.
** Corresponding author at: Department of Maxillofacial Biomedical Engineering and Institute of Oral Biology, School of Dentistry, Kyung Hee University, 1 Hoegi-dong, Dongdaemun-gu, Seoul 130-701, Republic of Korea.
E-mail addresses: yshwang@khu.ac.kr (Y.-S. Hwang), kdp@ajou.ac.kr (K.D. Park).
[1] These authors equally contributed to this work.

https://doi.org/10.1016/j.jiec.2019.01.017
1226-086X/

be closely related to proteolysis of collagen molecule, and various chemical treatments, such as succinylation, methylation and acetylation, have been applied to modify the collagen molecule in order to suppress its antigenicity and to control the rate of proteolysis [17].

In recent years, keratin, extracted from human hair, has received great attention as an alternative biomaterial due to its human source-derived excellent biocompatibility, potential for autologous transplantation and abundant availability, and has been applied for the management of skin wounds. Keratins are natural proteins classified as intermediate filaments generally found in epithelial cells in skin and hair, and are mainly composed of alpha-keratins, type I (acidic) keratin and type II (basic) keratin, to form a left-handed heterodimer helix by interacting with each other. The molecular weight of alpha-keratin monomers is known to be 40–50 kDa (type I) and 50–60 kDa (type II) [18]. Many reports have demonstrated that keratin treatment on the wound sites of an animal model accelerated re-epithelialization and subsequently more rapid wound healing. In addition, a highly accelerated wound healing effect was reported in a patient with recessive dystrophic epidermolysis bullosa by the treatment with keratin-based biomaterials [19,20]. These findings have significant implications for potential applications of keratin as biomaterials in wound healing. However, despite the well-proved effects of keratin in wound healing, most animal studies with keratin-based biomaterials in wound healing have used keratin extracted from sheep wool, and as such there is no underlying direct biological evidence for the biological function of hair keratin in skin regeneration. Furthermore, keratin is a highly hydrophobic protein composed of lots of hydrophobic amino acids including aromatic amino acids, proline, etc., which may indicate the poor solubility of keratin and limit its application in the fabrication of various types of biomaterials [21].

Therefore, in this study, for translational biomedical application of human hair keratin-based biomaterials in wound healing, *in situ* cross-linkable keratin hydrogels was designed and the cellular interaction of hair-derived keratin with human skin keratinocyte was studied by evaluating morphological change, proliferation, gene and molecular expression profiles related to epithelial-mesenchyme transition (EMT) and migration upon keratin treatment. In addition, the wound healing characteristics of the *in situ* forming hydrogel were evaluated using a mouse model with full-thickness skin defect.

Materials and methods

Extraction of human hair keratin

Human hair samples (50 g) were washed and rinsed thoroughly with 70% (v/v) ethanol and distilled water. Washed hair samples were then soaked in the mixture of chloroform and methanol (2:1; v/v) for 24 h to de-lipidize, after which they were air-dried. Human hair keratins were extracted according to a method published previously [22]. Briefly, delipidized hair was treated with 2% (v/v) peracetic acid (Sigma) at 37 °C for 24 h, and after washing with phosphate buffered saline (PBS), the hairs (20 g) were treated with 400 mL of Shindai solution containing 5% (v/v) 2-mercaptoethanol, 5 M urea, 2.6 M thiourea, 25 mM Tris pH 8.5 for 72 h while stirring at 300 rpm. The resulting mixture was centrifuged at 4,500 g for 20 min, and the supernatant was filtered through the filter paper with pore size 2.5 μm. The obtained solution was dialyzed using 12–14 kDa cutoff dialysis membrane (Spectra/Por®) against distilled water until 2-mercaptoethanol was not detected in dialysate using 5,5′-dithio-bis-(2-nitrobenzoic acid) (DTNB) method (Ellman's reagent) [23]. The resulting solution was then lyophilized to obtain keratin powder.

Fabrication of keratin-based in situ *forming hydrogel*

To improve water solubility of the keratin and induce *in situ* hydro-gelation, the extracted human hair keratin was chemically functionalized with poly(ethylene glycol) (PEG; Mn = 4000) and tyramine (TA). Briefly, horseradish peroxidase (HRP)-reactive keratin-PEG-TA polymer was synthesized through a two-step reaction: (1) terminal hydroxyl groups of PEG were conjugated with *p*-nitrophenylchloroformate (PNC) in the presence of triethylamine and 4-dimethylaminopyridine, and ethylenediamine and TA were then added to this PEG-diPNC solution as described in our previous reports [24,25]; (2) the amine-terminated PEG-TA was conjugated to carboxyl group of keratin via EDC/NHC coupling chemistry. The reaction was carried out for 24 h at room temperature, and the resulting solution was filtered, dialyzed using 12–14 kDa cutoff dialysis membrane (Spectra/Por®) against distilled water for 3 days, and lyophilized. The chemical structure of keratin-PEG-TA polymer was characterized using ^{1}H NMR (OXFORD instrument, AS400, UK), and keratin/PEG composition in keratin-PEG-TA polymer was determined using TGA (TA instrument, TGA Q50, USA), and the keratin to PEG ratio was 3:2 (w/w). The TA contents (degree of substitution, DS) of the polymer were measured quantitatively at 275 nm using a UV visible spectrophotometer (V-750 UV/vis/NIR, Jasco, Japan).

In situ forming keratin-based hydrogels were fabricated by simply mixing the modified keratin polymer with HRP and H_2O_2. The polymer was first dissolved in PBS (10 mM, pH 7.4) to a final concentration of 5 wt.%, and it was divided into two aliquots containing either HRP (0.2 mg/mL) or H_2O_2 (0.35 wt.%) (volume ratio of keratin-PEG-TA: HRP/H_2O_2 = 9:1). The mechanical stiffness (G′; elastic modulus, G″; viscous modulus) of hydrogels was confirmed using a rheometer (strain = 0.01%, frequency = 0.1 Hz).

Cell culture, cell viability assay and morphological observation

In this study, human keratinocyte cell line (HaCat cell line) was used to evaluate cellular interaction of human hair keratin, and HaCat cells were cultured in normal culture medium, high glucose-Dulbecco Modified Eagle Medium (DMEM; Gibco) supplemented with 10% FBS and 1% penicillin-streptomycin, in a humidified atmosphere of 5% CO_2 at 37 °C, and the medium was refreshed three times per week.

HaCat cells were seeded on a cell culture plate at a seeding density of 1×10^4 cells/cm^2, and, after 24 h of culture, HaCat cells were cultured in normal culture medium with or without 0.5(w/v)% keratin in a humidified atmosphere of 5% CO_2 at 37 °C, and the medium was refreshed every two days. After keratin treatment, the calcein-AM/ethidium homodimer Live/Dead assay (Invitrogen) was used to verify cell viability according to the manufacturer's instructions, and the HaCat morphology was observed using inverted fluorescent microscopy (Olympus IX71) and scanning electron microscope (SEM) (Hitachi S-2300, Hitachi Co. Ltd.). Briefly, HaCat cells were fixed with 4% paraformaldehyde (PFA) for 10 min, washed three times with PBS, and were then frozen and desiccated thoroughly. The samples were then mounted on a metal stub and coated with platinum using a sputter-coater (IB-3, Giko Engineering Co) operated at 15 kV for 5 min, and the images were captured.

Cell proliferation assay

Cell proliferation upon keratin treatment was measured using Cell Counting Kit-8 (Dojindo Laboratories). HaCat cells were seeded on a cell culture plate at a seeding density of 1×10^4 cells/cm^2, and cultured in normal culture medium with or without 0.5 (w/v)% keratin in a humidified atmosphere of 5% CO_2 at 37 °C, and

the medium was refreshed every two days. At specific time points (1, 2, 4 and 6 days), each well had 10 μL of the Cell Counting Kit-8 solution added and then was incubated at 37 °C for 2 h. Cell proliferation assays were performed in a 96-well plate reader by measuring the absorbance at a wavelength of 450 nm.

Immunocytochemical staining & fluorescence labeled keratin treatment

For immunocytochemical staining, HaCat cells during keratin treatment were fixed with 4% PFA for 10 min and then washed three times with PBS. The fixed HaCat cells were permeabilized with 0.1% triton X-100 (Sigma), and treated with 10% (w/v) normal goat serum (Invitrogen) in PBS to block non-specific binding of antibodies, and then incubated overnight at 4 °C with primary antibodies such as rabbit-anti-human E-cadherin antibody (Cell Signaling Tech), rabbit-anti-human vimentin antibody (abcam), and mouse-anti-human integrin β1 antibody (Santa cruz). Primary antibodies were detected with the secondary Alexa fluor 488 goat anti-rabbit antibody (Thermo scientific) or Alexa fluor 594 goat anti-mouse antibody (Thermo scientific) for 1 h at room temperature. The cells were counter-stained with 4′,6-diamidino-2-phenylindole (DAPI) to visualize the cell nucleus. Fluorescently labeled cells were imaged using inverted fluorescent microscopy (Olympus IX71).

In addition, in order to evaluate the cellular interaction of keratin with HaCat cells, the extracted keratin was labelled with fluorescence using the Alexa Fluor 488 protein labeling kit (Thermo Fisher) according to the manufacturer's instructions. HaCat cells were incubated for 24 h in normal culture medium with 0.5(w/v)% fluorescence labelled keratin in a humidified atmosphere of 5% CO_2 at 37 °C. After 24 h incubation, the cells were fixed with 4% PFA for 10 min and then washed three times with PBS. The fixed cells were permeabilized with 0.1% triton X-100, and treated with 10% (w/v) normal goat serum in PBS to block non-specific binding of antibodies, and then incubated overnight at 4 °C with TRITC conjugated anti-human F-actin (molecular probes). The cells were counter-stained with DAPI to visualize the cell nucleus. Fluorescently labeled cells were imaged using inverted fluorescent microscopy (Olympus IX71) and a confocal microscope (Olympus BX51).

Cell migration assay

The migration assay was done using Culture-Insert 2 well migration assay kit (Ibidi) according to the manufacturer's instructions. The HaCat cells were seeded within Culture-Insert 2 well on culture plates at a seeding density of 2×10^4 cells/cm^2, and cultured to reach confluency within insert wells for 2 days in normal culture medium, high glucose- DMEM supplemented with 10% FBS and 1% penicillin-streptomycin, in a humidified atmosphere of 5% CO_2 at 37 °C. After 2 days, one of the cell cultures was treated with 10 μg/ml of mitomycin C for 2 h to inhibit further proliferation, and then confluent cell layer was washed with PBS three times. The cells were incubated for 24 h in normal culture medium with or without 0.5(w/v)% keratin in a humidified atmosphere of 5% CO_2 at 37 °C, and migration activity of HaCat on space between insert wells was imaged using inverted fluorescent microscopy (Olympus IX71) and characterized by immunocytochemical staining using the same procedure described previously. The migrated distance was calculated with the pictures using a sigma-C plot program.

Gene and molecular expression assay

For reverse transcription-polymerase chain reaction (RT-PCR) analysis, the total RNA from the cultured cells was extracted by using TRIzol® reagent (Invitrogen). RNA samples were quantified using NanoDrop 1000 Spectrophotometer (Thermo Scientific), and RNA integrity was checked on 1% agarose gels using a 0.5X TAE buffer stained with SYBR® Safe DNA Dye (Invitrogen). cDNA was synthesized from 0.5 μg of total RNA per sample using PreMix kit (AccuPowerTM CycleScript RT PreMix (dT20), Bioneer) in a total volume of 20 μL. The reaction process was conducted at 37 °C for 30 s, at 48 °C for 4 min, at 55 °C for 30 s and at 95 °C for 5 min. The synthesized cDNA was reacted with the specific primers listed in Table 1, using the HiPi PCR PreMix Kit (Elpis Biotech) and subsequently amplified by RT-PCR system (Veriti®, applied biosystems). After denaturation at 95 °C for 5 min, the reactions were conducted at 95 °C for 3 s, 54–58 °C for 30 s, and 72 °C for 30 s for a total of 35 cycles. Amplified products were verified electrophoretically on 1.5% agarose gels. All reactions were performed in triplicate experiments. For quantitative analysis, the intensity of the bands was quantified with Image J (National Institutes of Health software) and normalized with respected to GAPDH.

For real time-qPCR, total RNA was extracted from cells using PureLinkTM RNA Mini Kit (Ambion). Neural gene expression was assessed through quantitative real-time polymerase chain reaction (qPCR) analysis using the Corbett RG6000 real time qPCR system (Quiagen). Amplifications were carried out in a final reaction volume of 20 μL with Power SYBR® Green PCR Master Mix (Applied Biosystems), 10 ng cDNA template, and 5 pmol primers. The sequences of the qPCR primers used were listed in Table 1. After denaturation at 50 °C for 2 min and 95 °C for 10 min, the reactions were conducted at 95 °C for 15 s, at 60 °C for 30 s, and at

Table 1
Primer sequences used in this study.

Primers for RT-PCR	Forward (5′ → 3′)	Reverse (5′ → 3′)
integrin αV	GTTGGGAGATTAGACAGAGGA	CAAAACAGCCAGTAGCAACAA
integrin α5	CATTTCCGAGTCTGGGCCAA	TGGAGGCTTGAGCTGAGCTT
integrin β1	TGTTCAGTGCAGAGCCTTCA	CCGGCTGGCCAAAGAGATGT
integrin β 6	CCGGCTGGCCAAAGAGATGT	AGTTAATGGCAAAATGTGCT
GAPDH	GAAGGTGAAGGTCGGAGT	GAGATGGTGATGGGATTTC
Primers for realtime-qPCR	Forward (5′ → 3′)	Reverse (5′ → 3′)
integrin αV	AATCTTCCAATTGAGGATATCAC	AAAACAGCCACTAGCAACAAT
integrin β5	GGAGCCAGAGTGTGGAAACA	GAAACTTTGCAAACTCCCTC
integrin β6	TCAGCGTGACTGTGAATATCC	GTGACATTTGGAGCTGTTCAC
fibronectin	CCCACCGTCTCAACATGCTTAG	CTCGGCTTCCTCCATAACAAGTAC
Snail	ACCACTATGCCGCGCTCTT	GGTCGTAGGGCTGCTGGAA
vimentin	AAAGTGTGGCTGCCAAGAACCT	ATTTCACGCATCTGGCGTTCCA
GAPDH	GGCATCGACTGTGGTCATGA	TGCACCACCAACTGCTTAGC

72 °C for 40 s for a total of 45 cycles, and relative quantification was then calculated. To confirm the amplification of specific transcripts, melting curve profiles were produced at the end of each PCR by cooling the sample to 40 °C and then heating it slowly to 95 °C while continuously measuring the fluorescence. A standard curve based on cycle threshold values was used to evaluate gene expression. In brief, 1:5 dilutions of known concentrations of cDNA in triplicate were used to generate curves extending from 50 pg to 80 ng of cDNA. Standard curves were generated for each gene including GAPDH as a control (housekeeping) gene. The relative amount of gene expression for each sample was normalized with respect to the control gene.

Wound healing animal test

To confirm the effect of keratin-based hydrogels on *in vivo* wound healing, we used male mice, C57BL/6J (Charles River Corp. Inc., Barcelona Spain) weighing 20–25 g. Fifteen healthy mice were obtained from an approved supplier, DBL. Co. Ltd., Korea. The mice were acclimated to the animal laboratory for one week. All experiments were conducted according to the Institutional Animal Care and Use Committee directives of Kwangwoon University. C57BL/6J mice were randomly divided into three groups. Groups 1 and 2 served as normal and negative control, and Group 3 was treated with keratin-based hydrogels. Five mice were used in each group, and the mice in each group were kept in individual cages. Wounds on mouse dorsal of Group 2 and 3 were created as previously described [26–28]. Briefly, mouse dorsal was clipped using a clipper to remove hair after anesthesia with isoflurane and the skin was disinfected with povidone-iodine followed by a rinse with 70% (vol/vol) ethanol. Skin folded with fingers after disinfection was punched using an 8-mm-diameter sterile biopsy punch to create two symmetrical full-thickness excisional wounds on either side of the midline. After creating the wounds, the area around each wound was carefully splinted using a 2-mm thick silicon donut-like splinting ring (12-mm-inner and 20-mm-outter diameter) to center the wound within the splint and to prevent self-contraction of the skin. For *in vivo* wound healing study, the keratin hydrogels were formed *in situ* on the exposed wound site using a dual syringe kit in which two different aliquots were separately loaded [29]. The polymers and other solutions were filtered using a syringe filter with a pore size of 0.2 μm for sterilization. Keratin-based hydrogels (100 μL) were placed into wound beds for Group 3 and the wounds were dressed and changed every other day with a transparent oxygen permeable wound dressing (Tegaderm film, 3 M). The mice of Group 2, the negative control, were treated with PBS in the same way. Wound closures in each mouse were observed using a stereo microscope (SZX16, Olympus) every other day and histological changes after 21 days were examined after staining with hematoxylin and eosin (H&E) to evaluate the wound healing effect of keratin-based hydrogel.

Statistical analysis

The results were presented as reflect the mean value ± standard deviation. ANOVA was performed to determine the statistical significance between the experimental groups, followed by student t-test to define the statistical difference between specific experimental variables with $p < 0.05$.

Results

Synthesis of in situ *forming keratin hydrogels*

The keratin was functionalized to generate injectable/sprayable hydrogel dressings that are formed *in situ* through HRP-catalyzed crosslinking reaction for wound healing application (Fig. 1A). To prepare HRP-reactive keratin derivative, NH_2-PEG-TA conjugate was first synthesized as described previously, and then NH_2-PEG-TA conjugates were grafted to carboxyl group of keratin using EDC/NHS coupling chemistry [24,25]. ^{1}H NMR spectra of NH_2-PEG-TA

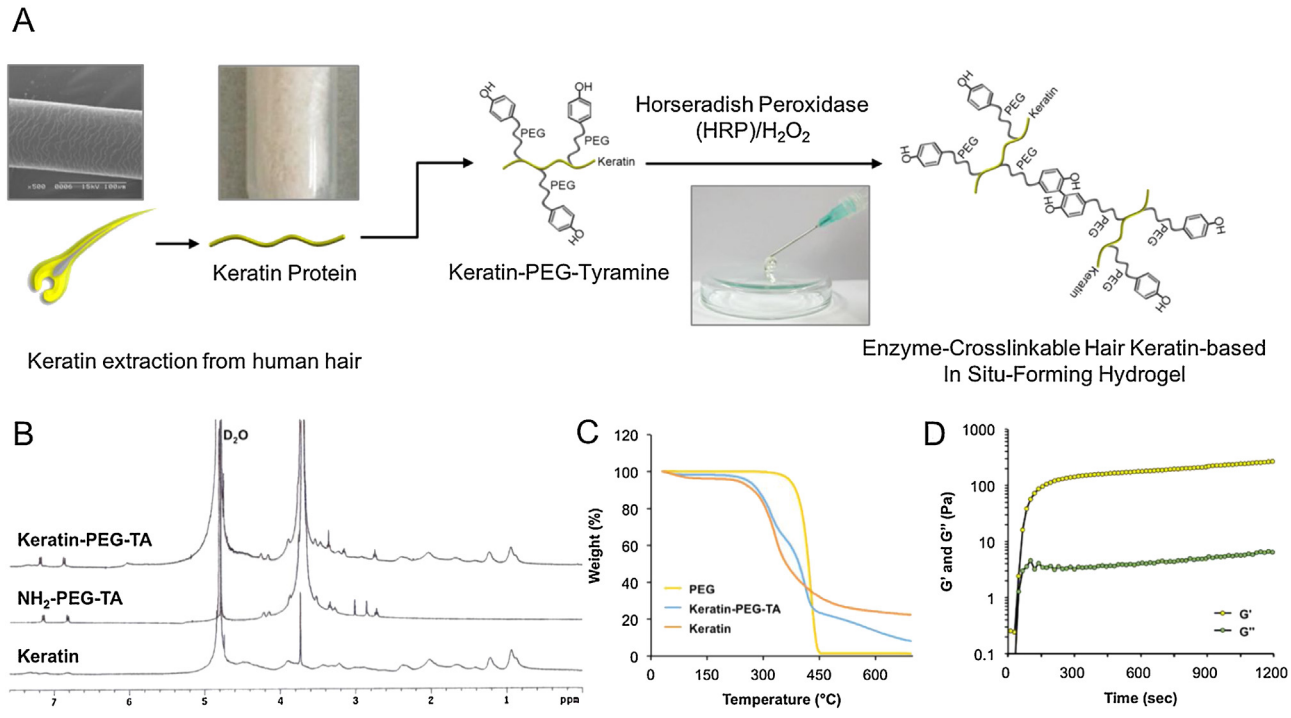

Fig. 1. Schematic illustration of the fabrication of keratin-based hydrogel and characterization of keratin-based hydrogel. (A) Schematic illustration of the development of enzyme crosslinkable keratin-based in situ forming hydrogel and its wound healing effect. (B) ^{1}H NMR spectra and (C) TGA curves of keratin, NH_2-PEG-TA, and keratin-PEG-TA conjugates. (D) Elastic modulus (G′) and viscous modulus (G″) of keratin-based hydrogels in presence of HRP (0.01 mg/mL) and H_2O_2 (0.0175 wt.%).

and keratin-PEG-TA showed characteristic peaks (ethylene group protons of PEG; δ 3.5–3.8, aromatic protons of TA; δ 6.8 and 7.2), indicating the successful grafting of PEG-TA to keratin backbone (Fig. 1B). The DS of TA in the polymer backbone was 477 μmol/g of polymer. In addition, it was confirmed by TGA that the weight ratio of keratin and PEG in keratin-PEG-TA was 3:2 (w/w) (Fig. 1C). Further, to test hydrogel formation and mechanical stiffness of keratin-based hydrogel, the elastic modulus (G′) and viscous modulus (G″) were analyzed by a rheometer. As shown in Fig. 1D, in the presence of HRP (0.01 mg/mL) and H_2O_2 (0.0175 wt.%), the sol-gel transition (cross point of G′ and G″ curves) rapidly occurred within 10 s, and the G′ reached 290 Pa. The hydrogel networks were formed *via* enzymatic cross-linking reaction of tyramine moieties in the polymer backbone through either C—C bonds between ortho-carbons of the aromatic ring or through C—O bonds between ortho-carbons and phenolic oxygen, as we previously reported [21]. After confirming *in situ* hydrogel fabrication, *in vitro* characterization of the effect of keratin on EMT and cell migration and the wound-healing efficacy of the keratin-based hydrogels were evaluated with a modified full thickness mouse excisional wound splinting model as previously described [27].

Keratin Induced Morphological Change of Human Keratinocyte

HaCat cells were treated with 0.5(w/v)% keratin extracted from human hair, and, after 1 and 3 days of culture, cell viability was evaluated by live/dead staining. As shown in Fig. 2A, there was no significant difference in cell viability between untreated HaCat cells and keratin-treated HaCat cells, and the HaCat cells exposed to 0.5(w/v)% keratin showed slightly decreased cell proliferation activity in comparison with untreated HaCat cell culture (Fig. 2B). In addition, the morphological change was obvious when HaCat cells were treated with 0.5(w/v)% keratin. The microscopic observation of untreated HaCat cells showed a denser and more organized cellular pattern in comparison with the keratin-treated HaCat cells, which gradually lost their regular morphology, organization pattern, and cell density. (Fig. 2C). Such morphological change was also found in live and dead staining, and also the morphological change of HaCat cells exposed to keratin to fibroblastic spindle shape was clearly observed in SEM analysis.

Keratin induced epithelial-mesenchyme transition of human keratinocyte

In order to visualize the interaction of keratin with HaCat cells, the extracted keratin was conjugated with a fluorescent dye, Alex Fluor 488, and HaCat cells were treated with Alex Fluor 488-conjuagated keratin. The fluorescence microscopic and confocal images showed fluorescent keratins attached on HaCat cells stained for phalloidin after 24 h of incubation (Fig. 3A). The keratin-mediated morphological change was further characterized by assessing EMT related molecular expressions such as vimentin, E-cadherin and integrin β1. The untreated HaCat cells with a dense and well-organized cellular pattern did not express vimentin, but

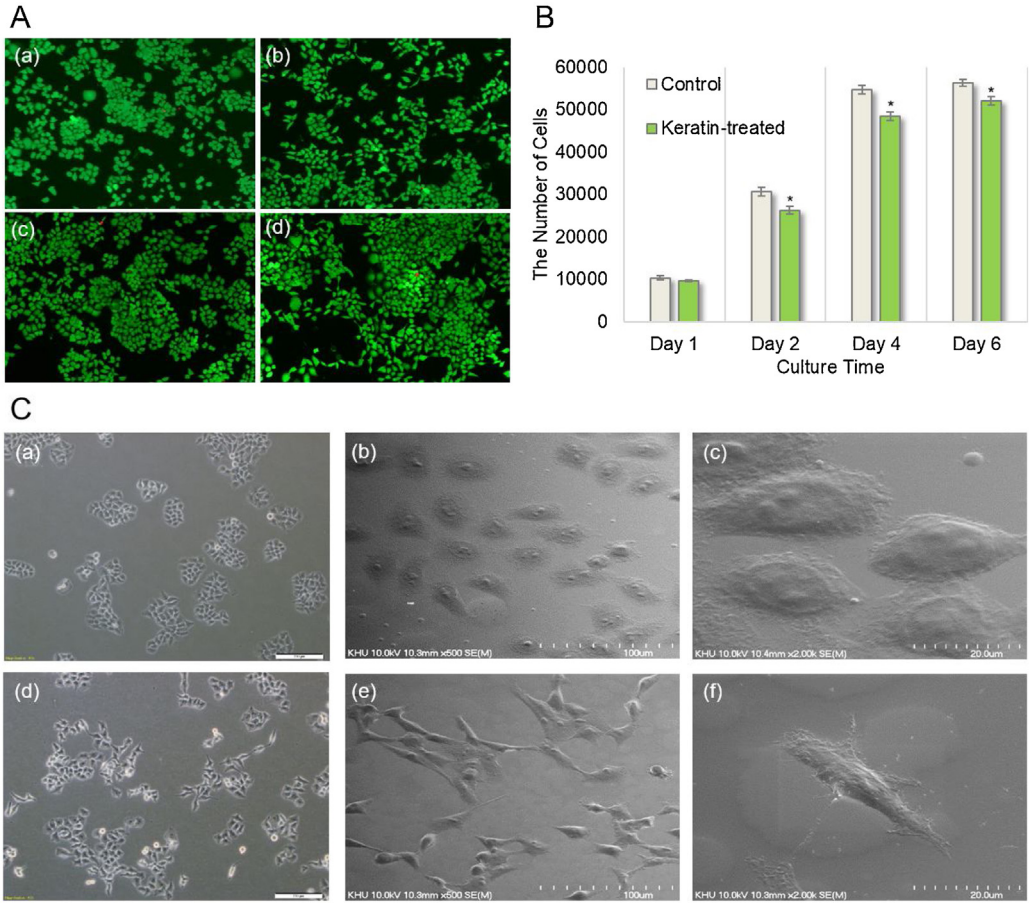

Fig. 2. Live and dead assay, cell proliferation assay and morphological observation for keratin-treated keratinocyte (HaCat). (A) live and dead assay of non-treated keratinocytes and keratin treated keratinocytes: non treated keratinocyte after 1 day (a) and 3 days (c) of culture, keratin treated keratinocyte after 1 day (b) and 3 days (d) of culture. (B) cell proliferation activity of non-treated keratinocytes and keratin-treated keratinocytes. (C) light microscopic and SEM observation of non-treated keratinocytes and keratin-treated keratinocytes after 3 days of culture: light microscopic image (a) and SEM images (b and d) of non-treated keratinocytes, light microscopic image (d) and SEM images (e and f) of non-treated keratinocytes. (n = 6, *: $p < 0.05$).

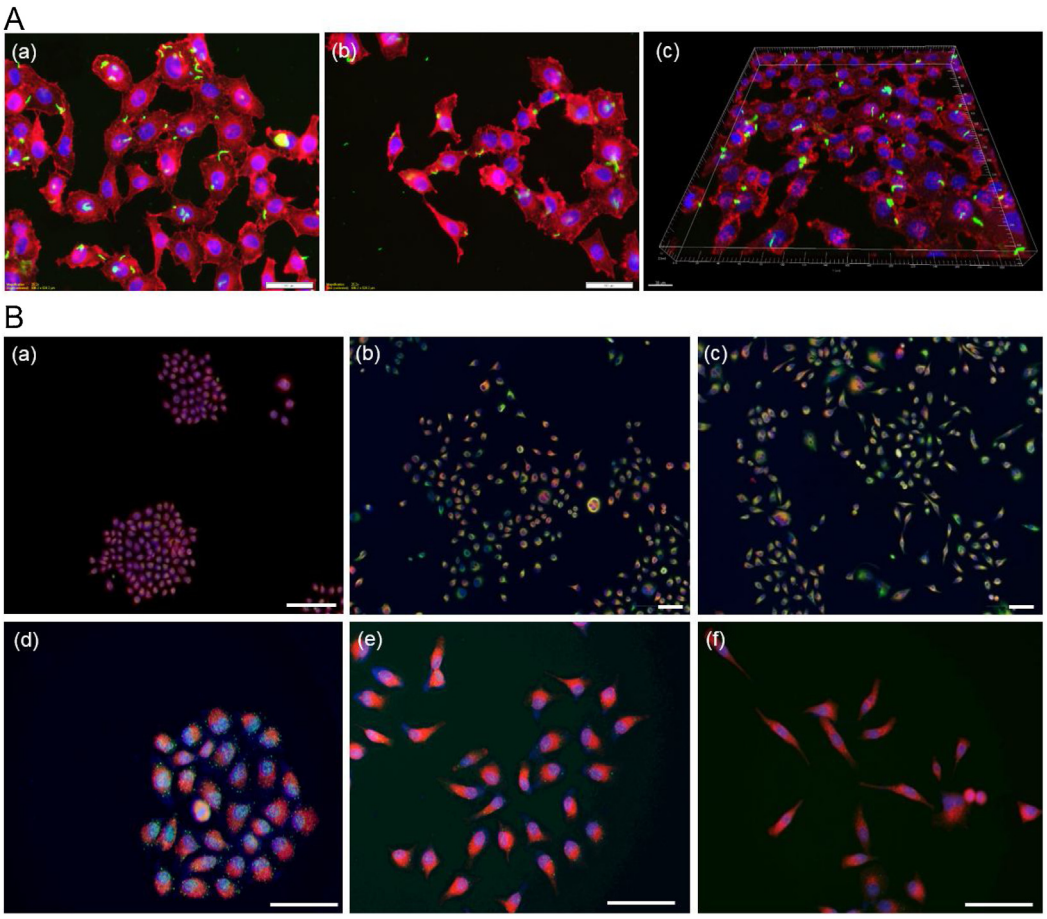

Fig. 3. Fluorescence microscopic and confocal microscopic observation of Alex Fluor 488-conjuagated keratin treated keratinocytes and immunocytochemical staining of EGF or keratin treated keratinocytes. (A) Fluorescence microscopic images (a and b) and confocal microscopic image (c) of keratinocytes treated with Alex Fluor 488-conjuagated keratin (green) after 24 h of culture and stained with TRITC-conjugated anti-human F-actin antibody (red). (B) Immunocytochemical staining of EGF or keratin treated keratinocytes: immunocytochemical stained images of vimentin (green) and integrin β1 (red) in non-treated keratinocytes (a), EGF-treated keratinocytes (b), and keratin-treated keratinocytes (c), and immunocytochemical stained images of E-cadherin (green) and integrin β1 (red) in in non-treated keratinocytes (d), EGF-treated keratinocytes (e), and keratin-treated keratinocytes (f) after 2 days of culture. (For interpretation of the references to colour in this figure legend, the reader is referred to the web version of this article.)

epithelial growth factor (EGF) or keratin treated HaCat cells showed a loosely organized pattern and a morphological change to fibroblastic spindle shape expressing vimentin strongly (Fig. 3B). In addition, as shown in immunostained images (Fig. 3B), control HaCat cells clearly showed the molecular expression of E-cadherin on the peripheral surface of cells, but EGF or keratin treated HaCat cells were found to lose the molecular expression of E-cadherin. There was no distinct difference in the molecular expression of integrin β1 between untreated and treated HaCat cells.

Keratin induced EMT-derived migration of human keratinocyte

EMT-related migration was also assessed using Culture-Insert 2 well migration assay, and the migration of HaCat Cells into the space between confluent cell colonies was evaluated. As shown in Fig. 4A, the cell population that migrated into space between confluent cell colonies did not show a distinct difference between untreated and keratin treated HaCat cells, but the migrated cell population in keratin treated HaCat cell culture showed a much stronger expression of vimentin and fibroblastic spindle shape. In contrast, the morphological change and molecular expression of vimentin were not found in the cell population of untreated HaCat cells in the space between confluent cell colonies (Fig. 4B). In order to prove EMT-related migration and to remove the possibility of proliferation, prior to keratin treatment and migration assay, HaCat cells losing proliferation capacity were prepared through mitomycin C treatment. Microscopic observation showed much higher cell population migrated into the space between confluent cell colonies in keratin treated HaCat cells in comparison with untreated HaCat cells (Fig. 4C). Such migrated cells in keratin treated HaCat cells showed the well-developed expression of vimentin and morphological change to fibroblast spindle shape (Fig. 4D). In addition, the mean of migrated distance was around 96 ± 23 μm and 174 ± 40 μm in mitomycin C treated HaCat cells and mitomycin C- and keratin-treated HaCat cells (Fig. 4E)

Keratin-mediated EMT and the following migration of HaCat cells were further characterized by assessing gene and molecular expression profile. RT-PCR analysis showed highly upregulated expressions of migration-related genes such as integrin αV, integrin α5, integrin β1, and integrin β6 in keratin treated HaCat cells (Fig. 5A), and quantitative real-time PCR also showed highly upregulated mRNA expressions of integrin αV, integrin β5, integrin β6, fibronectin, Snail and vimentin in EGF or keratin treated HaCat cells in comparison with untreated HaCat cells (Fig. 5B). Western blot analysis also indicated keratin treatment induced molecular expressions of integrin β1 and vimentin in EGF or keratin treated HaCat cells in comparison with untreated HaCat cells (Fig. 5C).

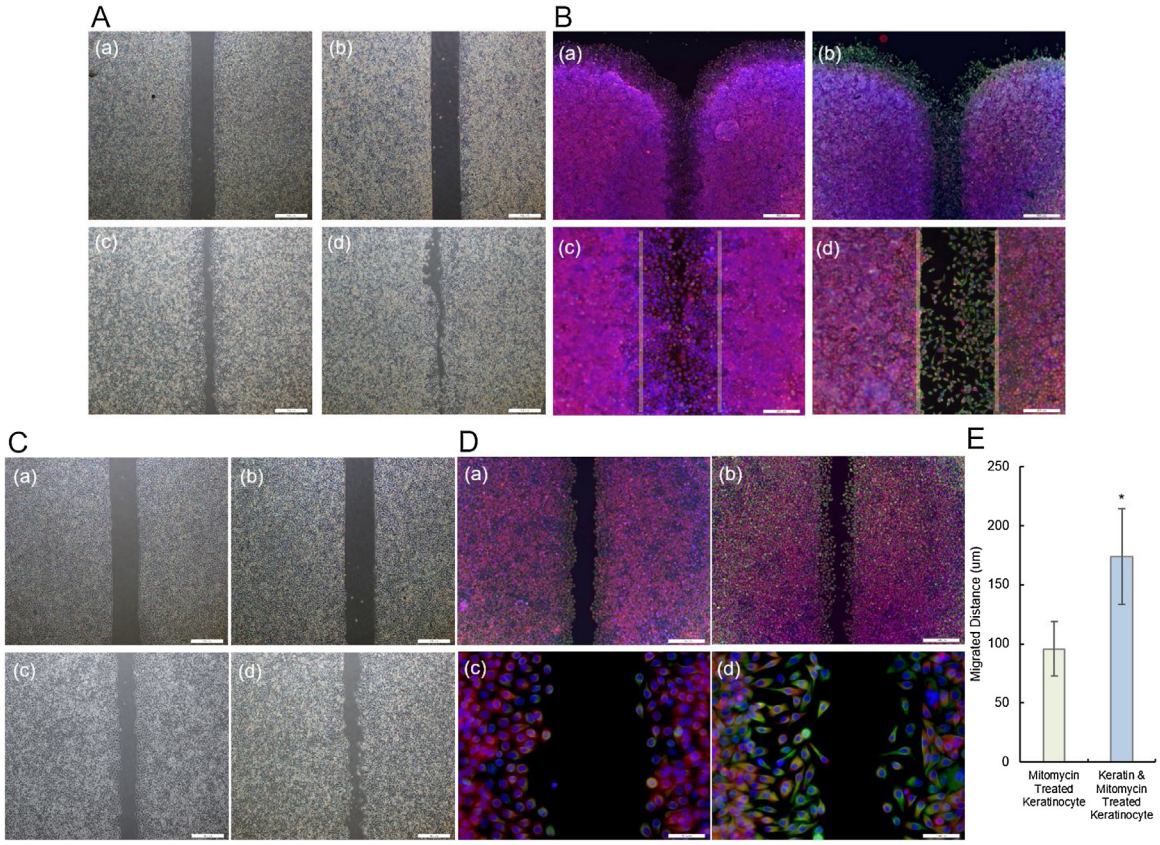

Fig. 4. Migration activity of non-treated and keratin-treated keratinocytes. (A) microscopic images of non-treated keratinocytes after 0 h (a) and 24 h (c) of migration assay and keratin-treated keratinocytes after 0 h (b) and 24 h (d) of migration assay. (B) Immunocytochemical stained images of vimentin (green) and integrin β1 (red) in non-treated keratinocytes after 0 h (a) and 24 h (c) of migration assay and in keratin-treated keratinocytes after 0 h (b) and 24 h (d) of migration assay. (C) microscopic images of mitomycin C-treated keratinocytes after 0 h (a) and 24 h (c) of migration assay and mitomycin C- treated and keratin-treated keratinocytes after 0 h (b) and 24 h (d) of migration assay. (D) Immunocytochemical stained images of vimentin (green) and integrin β1 (red) in mitomycin C-treated keratinocytes (a and c) after 24 h of migration assay and mitomycin C- treated and keratin-treated keratinocytes (b and d) after 24 h of migration assay. (E) Migrated distance of mitomycin C-treated keratinocytes and mitomycin C- treated and keratin-treated keratinocytes after 24 h of migration assay ($n = 10$, *: $p < 0.05$). (For interpretation of the references to colour in this figure legend, the reader is referred to the web version of this article.)

Keratin-based hydrogel treatment accelerated wound healing process

In animal test, each wound was observed for 21 days after post treatment, and wound closures in each group at day 21 were observed using a stereo microscope. As shown in Fig. 6A, skin aspect was fully recovered without any sign of scab and contraction of the skin in keratin-based hydrogel treated mice (Fig. 6A(d)), while scab in the skin was found to still be present on the wound bed in negative control group at day 21 (Fig. 6A(b)). To confirm the wound healing effect, the tissue slides were stained with H&E, and the wound healing efficacy was calculated by evaluating the rate of skin re-epithelialization, remodeling, and repair in each slide (Fig. 6B). The rates of re-epithelialization, remodeling, and repair in keratin-based hydrogel treated group were 2-fold higher than those of the negative control group, which were calculated as 50, 37.5 and 12.5% in the negative control group, and as 20, 50 and 30% in the keratin-based hydrogel treated group. As shown in Fig. 6B, the histological images of skin from mice treated with keratin-based hydrogel showed the re-epithelialization of skin with thick epidermis and the proliferation of dermal fibroblast with adnexa in dermis (Fig. 6B(d)), wound remodeling with skin adnexa and the proliferation of dermal fibroblast with skin adnexa and dense dermal fiber (Fig. 6B(e)), and complete wound repair with skin adnexa, regeneration of muscle tissue, and increased hair follicles (Fig. 6B(f)). On the other hand, the histological images of negative control represent the re-epithelialization of epidermis with slightly thin epidermis (Fig. 6B(a)), wound remodeling with less proliferation of dermal fibroblast and deposition of collagen than that of keratin-based hydrogel group (Fig. 6B(b)) in comparison with the skins of keratin-based hydrogel treated mice, and wound repair with skin adnexa, but with no muscle tissue found in the skin (Fig. 6B(c)). The overall rate of the wound healing process in the keratin-based hydrogel treated group was significantly high in comparison with the negative control group. These results indicate that the remodeling of tissues through rapid re-epithelialization is faster in the keratin-based hydrogel treated group than in the negative control group, and eventually the rate of tissue repair was also significantly increased in the keratin-based hydrogel treated group.

Discussion

The keratin-based hydrogel was fabricated by the conjugation of TA-conjugated PEG to keratin molecule *via* a slight modification of a previously reported method [25]. The sol-gel transition was processed within 10 sec, and the hydrogel formation could be formed rapidly in the presence of HRP and H_2O_2 (Fig. 1A).

Wound healing is a complex biological process, and includes dermal contraction and keratinocyte migration to restore the skin's integrity. Epithelial-mesenchyme transition, migration of keratinocyte and reepithelization into the wound site are essential to restore the epidermis and barrier function at the early stage of the wound healing process after skin injury [30]. This keratinocyte migration is known to be regulated by cell to soluble growth factor

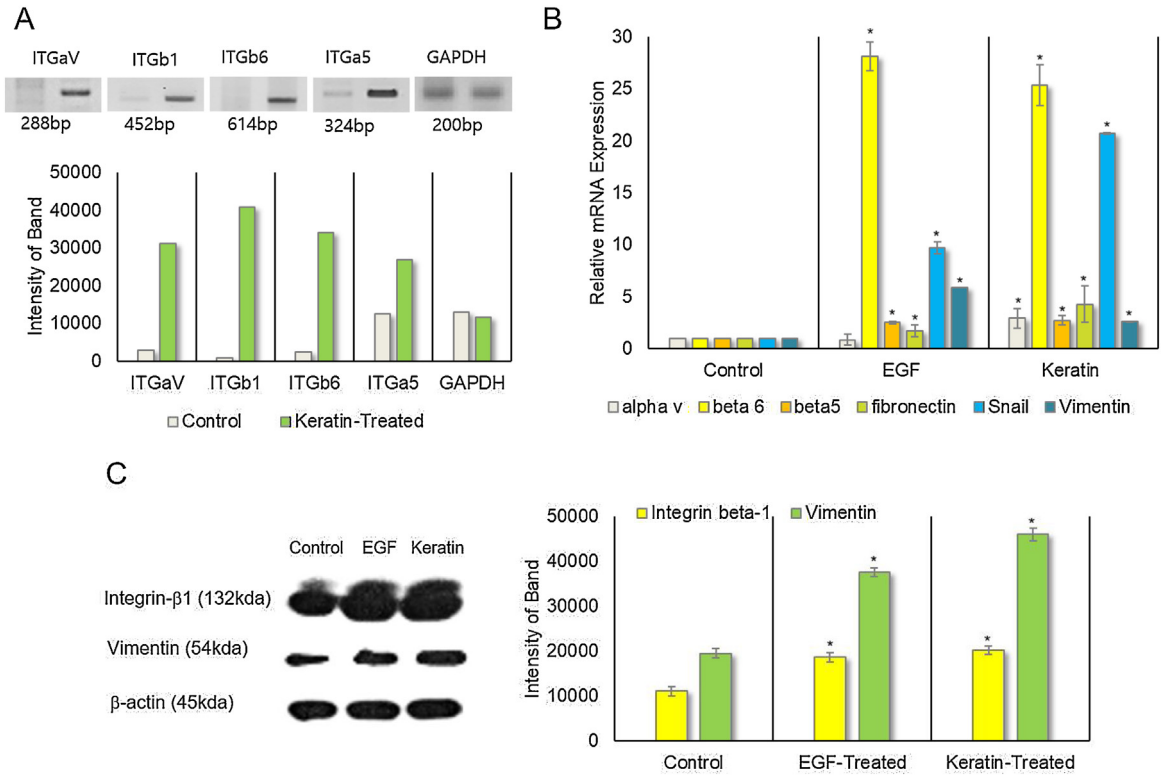

Fig. 5. Gene and molecular expression profile. (A) RT-PCR analysis of integrin αV, integrin α5, integrin β1, integrin β6 and GAPDH in non-treated keratinocytes and keratin-treated keratinocytes after 2 days of culture. (B) Quantitative analysis of mRNA expressions of integrin αV, integrin β5, integrin β6, fibronectin, snail and vimentin in non-treated keratinocytes, EGF-treated keratinocytes and keratin-treated keratinocytes after 2 days of culture. (C) Western blot analysis for molecular expressions of integrin β1 and vimentin in non-treated keratinocytes, EGF-treated keratinocytes and keratin-treated keratinocytes after 2 days of culture. (n = 4, *: $p < 0.05$: the statistical values were estimated by comparing experimental groups with non-treated control group).

interaction and cell to extracellular matrix (ECM) interaction, and much is known about the cellular interaction of keratinocyte, as keratinocytes sense and interact with various ECM components, such as type I collagen, type III collagen, type IV collagen, fibronectin, laminin, etc., using specific integrin receptors [31]. This knowledge has led researchers to use ECM component, particularly collagen, as biomaterials to enhance the wound healing process. However, although many clinical studies have reported highly accelerated wound healing after treatment of various keratin-based biomaterials, less is known about how hair-derived keratins interact with cells and enhance the wound healing process.

In this study, microscopic and electron microscopic observation showed that keratin treatment induced morphological change of keratinocyte to an elongated spindle shape, which is consistent with the report that migrating keratinocyte was found to become elongated at the initiation of migration in wound healing [32]. This morphological change was accompanied by a change of gene and molecular expressions in keratinocytes upon keratin treatment. Immunocytochemical staining showed the loss of E-cadherin, a key cell-cell adhesion molecule to regulate intercellular junction organization [33], expressions at the cell periphery of keratinocytes escaped from cell colonies with organized pattern, and fibroblastic spindle shaped cells showed highly upregulated expression of vimentin upon keratin treatment (Fig. 3C). With the loss of E-cadherin expression, vimentin expression is a marker of the epithelial to mesenchymal transition (EMT), the process by which epithelial cells lose their polarity and cell to cell adhesions to neighboring cells and differentiate into mesenchymal cells, and the level of vimentin expression was found to be correlated with mesenchymal cell morphology and motility.[34] The keratin-induced EMT process was also characterized by slightly decreased proliferation activity of keratinocytes in cell proliferation assay (Fig. 3B), which is consistent with the proliferation arrest during EMT process of keratinocyte.[35] As also shown in Figs. 3 and 5, the increased gene and molecular expressions of Snail, known as a transcription factor to control EMT by suppressing E-cadherin expression [36], and the mesenchymal markers such as fibronectin and vimentin [37] proved keratin-treated keratinocyte was undergoing an EMT process.

EMT is known to be commonly associated with increased cell migration [38]. In this study, migration assay was done using keratinocyte losing proliferation activity via mitomycin C treatment in order to distinguish between proliferation and migration. The migration assay showed the increased migration activity of keratin-treated keratinocytes, and the migrated keratinocyte showed fibroblastic spindle morphology and vimentin expression, which indicated that the migrated keratinocyte underwent an EMT process (Fig. 4). With various gene and molecular expressions indicating EMT such as vimentin, fibronectin and snail (Figs. 4 and 5), mRNA expressions of several integrin classes participating in keratinocyte migration such as integrin αV, integrin α5, integrin β1, and integrin β6 were found to be highly upregulated in keratin-treated keratinocytes (Fig. 5). Integrin αVβ6 is known to be expressed in various epithelial cells and to mediate dynamic processes including cell migration of keratinocyte in wound healing [39], and also keratinocyte migration on fibronectin was proved to be controlled by integrin α5β1 [40]. Taken together with all these findings, our results show that hair-derived keratin protein induced EMT and the subsequent migration of keratinocytes.

Based on these findings for cellular interaction of keratin in terms of keratinocyte migration, for the efficient application of keratin protein as biomaterials for wound healing, keratin based *in*

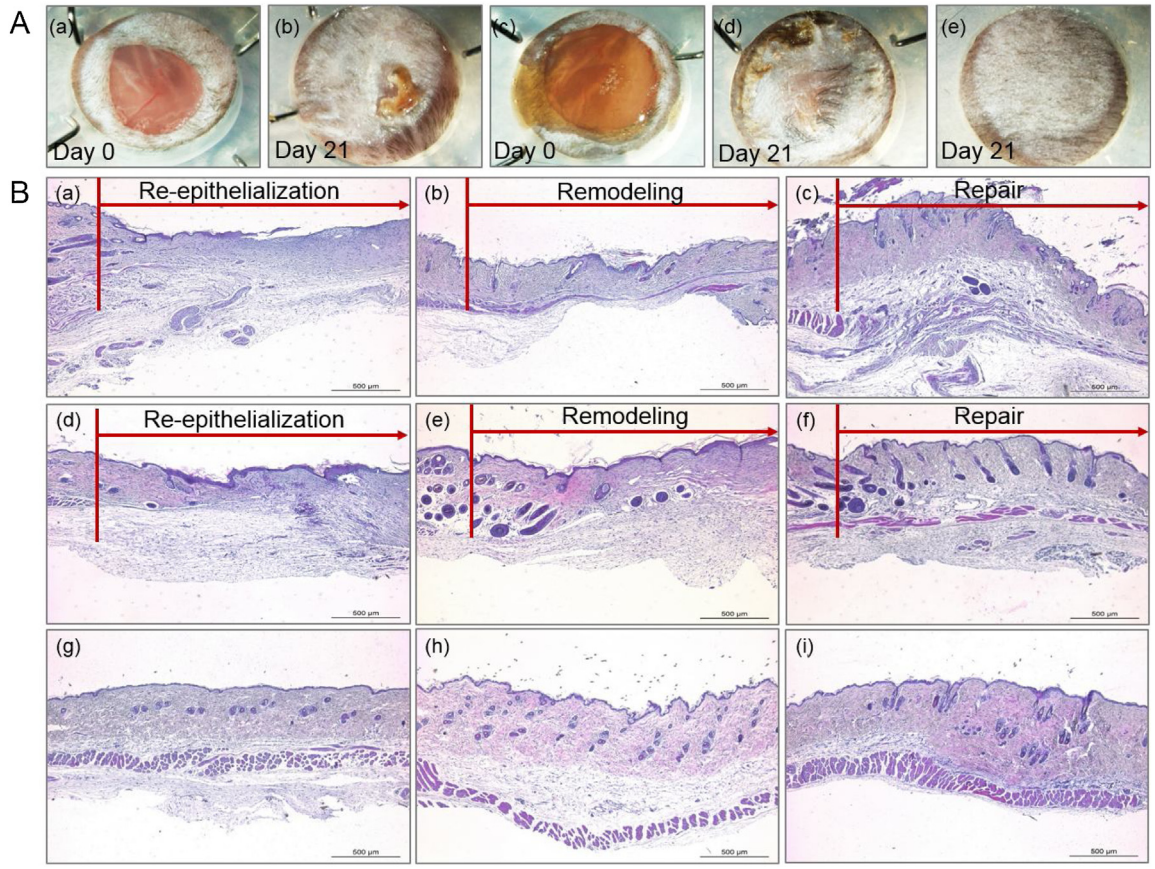

Fig. 6. Wound healing effect of keratin-based hydrogels in the full thickness mouse excisional wound splinting model. (A) Stereo microscopic images of wound sites of non-treated mouse (negative control: a and b), keratin-based hydrogel-treated mouse (c and d), and natural skin of mouse (e) at day 0 and day 21 in post wounding. (B) Histological images of hematoxylin and eosin (H&E) staining of non-treated skin (negative control, (a–c)), keratin-based hydrogels treated skin (d–f), and natural skin (g–i). Representative images of H&E stained histological sections at day 21 after post-wounding show that keratin-based hydrogel treatment promoted wound healing with complete skin appendage regeneration in comparison with negative control. Scale bars represent 500 μm.

situ forming hydrogel was applied to *in vivo* animal models. To evaluate the effect of keratin-based hydrogel on wound healing, a full thickness wound area in mouse was fully covered with keratin-based hydrogels. As shown in Fig. 6, the animal study with the full thickness mouse model showed keratin-based hydrogel highly accelerated re-epithelialization, remodeling, and repair, which are known as the classic wound healing phases [41]. The accelerated wound healing process might be closely related to the positive function of human hair-derived keratin in EMT and the migration of keratinocytes. In addition, the released content of H_2O_2 in keratin-based hydrogel was approximately 500 μM in 24 h incubation (data not shown), and the H_2O_2 released from keratin-based hydrogel might positively influence the accelerated wound healing together with keratin. It is well known that reactive oxygen species such as H_2O_2 are generated in wound healing and increase tissue vascularization by inducing the expression of the angiogenic form of vascular VEGF [42]. However, the biological function of the released H_2O_2 in our keratin-based hydrogel needs to be studied further for a better understanding of the wound healing process.

Conclusion

In this study, *in situ* cross-linkalble keratin-based hydrogels were developed using keratin extracted from human hair. *In vitro* studies demonstrated that EMT and EMT-related migration of keratinocytes could be induced by keratin treatment. Based on the finding of such cellular interaction of keratin, keratin-based *in situ* forming hydrogel was developed and applied to *in vivo* wound models, demonstrating that wound healing process was also accelerated by the treatment with keratin-based hydrogel. Taken together, our study suggests that human hair-derived keratin-based hydrogels can be assumed to be a suitable biomaterial for skin and tissue regeneration.

Disclosures

The authors declare that they have no conflict of interest.

Acknowledgements

This work was supported by the National Research Foundation of Korea (NRF) grant funded by the Korea government (MSIP) (NRF-2015M3A9E2028578, NRF-2010-0027963, NRF-2016R1D1A1B03931933 and NRF-2017-01410002).

References

[1] D.E. Fullenkamp, J.G. Rivera, Y.K. Gong, K.H. Lau, L. He, R. Varshney, P.B. Messersmith, Biomaterials 33 (2012) 3783.
[2] M.A. Fonder, G.S. Lazarus, D.A. Cowan, B. Aronson-Cook, A.R. Kohli, A.J. Mamelak, J. Am. Acad. Dermatol. 58 (2008) 185.
[3] Y. Lee, K.H. Choi, K.M. Park, J.M. Lee, B.J. Park, K.D. Park, ACS Appl. Mater. Interfaces 9 (2017) 16890.
[4] N.Q. Tran, Y.K. Joung, E. Lih, K.D. Park, Biomacromolecules 12 (2011) 2872.
[5] A. GhavamiNejad, C.H. Park, C.S. Kim, Biomacromolecules 17 (2016) 1213.
[6] M.C. Giano, Z. Ibrahim, S.H. Medina, K.A. Sarhane, J.M. Christensen, Y. Yamada, G. Brandacher, J.P. Schneider, Nat. Commun. 5 (2014) 4095.

[7] L. Mi, H. Xue, Y. Li, S. Jiang, Adv. Funct. Mater. 21 (2011) 4028.
[8] K.M. Park, S. Gerecht, Nat. Commun. 5 (2014) 4075.
[9] S. Park, K.M. Park, Biomaterials 182 (2018) 234.
[10] S.E. Mutsaers, J.E. Bishop, G. McGrouther, G.J. Laurent, Int. J. Biochem. Cell Biol. 29 (1997) 5.
[11] I. Pastar, O. Stojadinovic, N.C. Yin, H. Ramirez, A.G. Nusbaum, A. Sawaya, S.B. Patel, L. Khalid, R.R. Isseroff, M. Tomic-Canic, Adv. Wound Care (New Rochelle) 3 (2014) 445.
[12] C.J. Doillon, C.F. Whyne, S. Brandwein, F.H. Silver, J. Biomed. Mater. Res. 20 (1986) 1219.
[13] K. Lin, D. Zhang, M.H. Macedo, W. Cui, B. Sarmento, G. Shen, Adv. Funct. Mater. (2018) 1804943.
[14] M. Mian, F. Beghe, E. Mian, Int. J. Tissue React. 14 (1992) 1.
[15] L.R. Ellingsworth, F. DeLustro, J.E. Brennan, S. Sawamura, J. McPherson, J. Immunol. 136 (1986) 877.
[16] R.J. Siegle, J.P. McCoy, W. Schade, N.A. Swanson, Arch. Dermatol. 120 (1984) 183.
[17] A.M. Diamond, S.D. Gorham, D.J. Etherington, J.G. Robertson, N.D. Light, Matrix 11 (1991) 321.
[18] H. Lee, K. Noh, S.C. Lee, I.-K. Kwon, D.-W. Han, I.-S. Lee, Y.-S. Hwang, Tissue Eng. Regen. Med. 11 (2014) 255.
[19] P.M. Pechter, J. Gil, J. Valdes, M. Tomic-Canic, I. Pastar, O. Stojadinovic, R.S. Kirsner, S.C. Davis, Wound Repair Regen. 20 (2012) 236.
[20] M.P. Than, R.A. Smith, S. Cassidy, R. Kelly, C. Marsh, A. Maderal, R.S. Kirsner, J. Dermatol. Treat. 24 (2013) 290.
[21] P. Staroń, M. Banach, Z. Kowalski, A. Staroń, Proc. ECOpole 8 (2014).
[22] H. Lee, Y.-S. Hwang, H.-S. Lee, S. Choi, S.Y. Kim, J.-H. Moon, J.H. Kim, K.C. Kim, D.-W. Han, H.-J. Park, Macromol. Res. 23 (2015) 300.
[23] P.M. Schrooyen, P.J. Dijkstra, R.C. Oberthur, A. Bantjes, J. Feijen, J. Agric. Food Chem. 48 (2000) 4326.
[24] Y. Lee, K.M. Park, J.W. Bae, K.D. Park, Colloids Surf. B Biointerfaces 102 (2013) 585.
[25] K.M. Park, K.S. Ko, Y.K. Joung, H. Shin, K.D. Park, J. Mater. Chem. 21 (2011) 13180.
[26] J.D. Luo, Y.Y. Wang, W.L. Fu, J. Wu, A.F. Chen, Circulation 110 (2004) 2484.
[27] X. Wang, J. Ge, E.E. Tredget, Y. Wu, Nat. Protoc. 8 (2013) 302.
[28] J. Asai, H. Takenaka, K.F. Kusano, M. Ii, C. Luedemann, C. Curry, E. Eaton, A. Iwakura, Y. Tsutsumi, H. Hamada, S. Kishimoto, T. Thorne, R. Kishore, D.W. Losordo, Circulation 113 (2006) 2413.
[29] Y. Lee, J.W. Bae, J.W. Lee, W. Suh, K.D. Park, J. Mater. Chem. B 2 (2014) 7712.
[30] M.M. Santoro, G. Gaudino, Exp. Cell Res. 304 (2005) 274.
[31] E.A. O'Toole, Clin. Exp. Dermatol. 26 (2001) 525.
[32] G. Odland, R. Ross, J. Cell Biol. 39 (1968) 135.
[33] M.J. Wheelock, P.J. Jensen, J. Cell Biol. 117 (1992) 415.
[34] M.G. Mendez, S. Kojima, R.D. Goldman, FASEB J. 24 (2010) 1838.
[35] K. Räsänen, A. Vaheri, J. Dermatol. Sci. 58 (2010) 97.
[36] A. Cano, M.A. Perez-Moreno, I. Rodrigo, A. Locascio, M.J. Blanco, M.G. del Barrio, F. Portillo, M.A. Nieto, Nat. Cell Biol. 2 (2000) 76.
[37] C. Yan, W.A. Grimm, W.L. Garner, L. Qin, T. Travis, N. Tan, Y.-P. Han, Am. J. Pathol. 176 (2010) 2247.
[38] R. Kalluri, R.A. Weinberg, J. Clin. Invest. 119 (2009) 1420.
[39] X. Huang, J. Wu, S. Spong, D. Sheppard, J. Cell Sci. 111 (1998) 2189.
[40] J.P. Kim, K. Zhang, J.D. Chen, K.C. Wynn, R.H. Kramer, D.T. Woodley, J. Cell Physiol. 151 (1992) 443.
[41] J.V. Quinn, Tissue adhesives in clinical medicine, PMPH-USA, 2005.
[42] S. Roy, S. Khanna, C.K. Sen, Free Radic. Biol. Med. 44 (2008) 180.